

FP 30

# CCD photometry in modern astronomy

Responsible MPIA staff contact: Jörg-Uwe Pott  
jpott@mpia.de

MPI for Astronomy  
Königstuhl 17  
69117 Heidelberg

Version 4.0.3, 10.08.2017

This manual is the product of the contribution of various students:

N. Krieger, M. Riener, S.M. Birkmann, E. Krmpotic, S. P. Quanz, M.  
Schartmann, K. Tristram, Jochen Tackenberg, Liyu Ambachew,  
Johannes Esser, Hector Hiss, & Michael Rugel

Please keep up this spirit, and contribute improvements!

# Contents

<b>1</b>	<b>Introduction</b>	<b>4</b>
<b>2</b>	<b>Fundamental principles</b>	<b>7</b>
2.1	Detectors . . . . .	7
2.2	Observations . . . . .	8
2.3	Data Reduction . . . . .	9
2.3.1	Bias . . . . .	10
2.3.2	Flat-field . . . . .	10
2.4	Basic principles of photometry . . . . .	10
2.5	The Hertzsprung-Russel-Diagramm . . . . .	14
2.5.1	Shift of the main sequence . . . . .	14
2.6	Stellar clusters . . . . .	15
<b>3</b>	<b>Layout of the experiment</b>	<b>18</b>
3.1	Hardware . . . . .	18
3.2	Software . . . . .	19
3.2.1	IRAF . . . . .	21
3.2.2	SAO-Image DS9 . . . . .	24
<b>4</b>	<b>Characterization of the CCD</b>	<b>26</b>
4.1	Preparations . . . . .	26
4.2	Properties of the dark current . . . . .	27
4.2.1	Theoretical background . . . . .	27
4.2.2	Execution of the measurements . . . . .	28
4.2.3	Analysis . . . . .	28
4.2.4	Tasks and discussion points for the protocol . . . . .	29
4.3	Flat-field correction . . . . .	29
4.3.1	Execution of the measurements . . . . .	29
4.3.2	Analysis . . . . .	31
4.3.3	Tasks and discussion points for the protocol . . . . .	31
4.4	Linearity and dynamical range of the CCD . . . . .	32
4.4.1	Execution of the measurements . . . . .	32
4.4.2	Analysis . . . . .	32
4.4.3	Tasks and discussion points for the protocol . . . . .	32
4.5	Sensitivity of the detector and noise properties . . . . .	34
4.5.1	Execution of the measurements . . . . .	35
4.5.2	Analysis . . . . .	35
4.5.3	Tasks and discussion points for the protocol . . . . .	36
<b>5</b>	<b>Color Magnitude Diagram</b>	<b>37</b>
5.1	Zeropoint calibration . . . . .	37
5.2	PSF photometry with STARFINDER . . . . .	38
5.2.1	Using STARFINDER . . . . .	39

5.3	Cross-match the PSF fitting results . . . . .	41
5.4	Plotting the CMD . . . . .	41
5.4.1	Tasks and discussion points for the protocol . . . . .	41
<b>6</b>	<b>Scientific observations</b>	<b>43</b>
6.1	Tasks . . . . .	43
6.2	Execution of the observations . . . . .	43
6.3	Analysis . . . . .	43
6.3.1	Introduction . . . . .	43
6.3.2	Data acquisition . . . . .	44
6.3.3	Bias . . . . .	44
6.3.4	Flatfield . . . . .	44
6.3.5	Finding the focus . . . . .	45
<b>7</b>	<b>Data Analysis</b>	<b>47</b>
7.1	Raw data reduction . . . . .	47
7.1.1	Execution . . . . .	47
<b>8</b>	<b>Command line commands for reading out the CCD</b>	<b>48</b>
8.1	Resetting the electronics . . . . .	48
8.2	Taking a dark exposure . . . . .	48
8.3	Taking a flatfield or science exposure . . . . .	49

# 1 Introduction

The results of astronomical research contribute significantly to the picture we have of our universe and are of great relevance to many areas in physics as they allow the study of matter under extreme conditions not reproducible on Earth. However, the analysis of these distant celestial objects requires special, complex methods. Large telescopes equipped with highly sensitive detectors are needed to measure the electromagnetic waves originating from these distant objects. In the optical wavelength range (wavelengths from 300 to 700 nm) most commonly semiconductor detectors (so called charged coupled devices, CCDs) are used for this purpose. The high quantum efficiency of these detectors enables to detect up to 9 of 10 incident photons. A detailed understanding of the instrumentation, the elaborate measurement techniques, and the complex data analysis procedures is therefore essential for the astrophysical interpretation of the data.

The Max-Planck-Institut für Astronomie (MPIA) provides a powerful CCD camera for the use in one of the laboratory courses of the physics department of the Ruprechts-Karls-Universität Heidelberg. The camera is attached to the institute's 70 cm KING (Königstuhl Instrument for Night sky Gazing) telescope. In the first part of the experiment fundamental properties of the detector will be analysed, such as the behaviour of the dark current, linearity, dynamical range, and quantum efficiency. Important characterising quantities will be determined and compared to other detection devices.

For the second part of the experiment observations of a star cluster in two optical spectral bands will be analysed and interpreted. The astronomical data analysis package IRAF<sup>1</sup> (Image Reduction and Analysis Facility) will be used to minimize artefacts in the raw data and a photometrical calibration of the data will be performed to produce a colour magnitude diagram. This diagram, very similar to the “Hertzsprung-Russell” diagram, is one of the most important tools in stellar astronomy as it provides the means to determine basic parameters of a stellar population. For the star cluster used in this experiment the distance and the age have to be determined.

The experiment “CCD Photometry” demonstrates basic methods of astronomical observation and analysis. It gives an insight into the telescope and detector technology used in modern astronomy, with special focus on optics, semiconductor physics, cryogenics, and vacuum technology. The work with the telescope provides an authentic experience of astronomical observations and research. The analysis of the telescope data is based on Poisson statistics and shows the fundamental limits in detecting stochastic processes. An understanding of these processes and a critical evaluation of the data are of large importance to signal processing in all fields of science.

The experiment is scheduled to take place on four afternoons (or two full days) possibly including one evening for the night-time observations if weather permits. Since clear weather is needed for the observations the planning is flexible and

---

<sup>1</sup><http://iraf.noao.edu/>

students are encouraged to contact the supervisors in advance to agree on a time schedule. Unfortunately, the climatic conditions on the Königstuhl mountain are not very favourable to sensitive astronomical observations and only a few nights of the year can be used for astronomical observations. The lab course can be completed without the night time experience.

An understanding of fundamental astronomical concepts (content of the lectures “Introduction into Astronomy and Astrophysics”) is required for the participation in this experiment. Expertise in electronic data analysis and especially Linux (e.g. scripting) are of great advantage<sup>2</sup>. For the preparation of the experiment students are advised to read the following book chapters in addition to these instructions:

- Chapter 6 and 7 of Léna et al.: “Observational Astrophysics” (Léna et al., 1998)
- Chapter 5 and 6 in Unsöld, Baschek: “Der neue Kosmos” (Unsöld & Baschek, 2002).

The knowledge of this information (especially on the functionality of the CCD detectors, on the data reduction process and on the significance of the Hertzsprung-Russell-Diagram) will be verified in an oral discussion at the beginning of the experiment. Due to the high complexity of the experiment and the tight schedule, a poor preparation can prolong the execution of the experiment significantly and can lead to the rejection of the students. A careful preparation is therefore absolutely imperative!

The experiment takes place at the Max-Planck-Institut für Astronomie (MPIA), Königstuhl 17, in the eastern dome on the Elsässer-Labor situated to the south of the main institute. Directions can be found on the homepage of the institute: <http://www.mpia.de/anfahrt>.

The following instructions are divided into three main parts: First (section 2) a few fundamental principles are reviewed to ensure the basic comprehension for the experiment. The delineation in the context of this manuscript is, however, not to be considered exhaustive. The second part (section 3) contains a description of the instrumental setup. The third and main part (sections 4 and 5) comprises the problems to be approached as well as the instructions for the execution of the tasks. The instructions conclude with requirements and tips for the concluding report and an appendix with more in-depth information on the software used for this experiment.

Further web resources are

- MPIA house telescope:  
<https://svn.mpia.de/trac/gulli/king/wiki/WikiStart>
- FP30 at MPIA:  
<https://svn.mpia.de/trac/gulli/king/wiki/WikiStart/FP30Doc>

---

<sup>2</sup>You will be faster and require less help from your supervisor. Successfully completing the experiment is also possible with little Linux or terminal/konsole experience.

- Official info on the lab course and its grading system (only in german but web translate works):  
<http://www.physi.uni-heidelberg.de/Einrichtungen/FP/info/betreuerhinweise.php>

## 2 Fundamental principles

### 2.1 Detectors

In astronomy it is not possible to investigate celestial objects in controlled laboratory conditions. Almost all of our knowledge about the universe comes from measurements of the electromagnetic waves emitted from various forms of matter in space. The intensity of this radiation is very small due to the large distances in the universe<sup>3</sup>. Typical radiation fluxes have intensities of  $10^{-29} \text{ W m}^{-2} \text{ Hz}^{-1} = 1 \text{ mJy}$ <sup>4</sup> in radio astronomy or a few photons per  $\text{m}^2$  and second in the optical wavelength range.

It goes without saying that the instrumentation used for the detection of radiation is of great significance for astronomy. In optical astronomy (wavelengths between 300 nm und 700 nm) photographic plates played an important role since their invention in the early 19th century. This completely changed about 35 years ago with the introduction of semiconductor detectors. These devices make use of the photoelectric effect to convert the arrival of photons on the detectors into electrons that are then collected in condensators and read out. These so called charged coupled devices (CCD) are the standard tool for the observing astronomer and it is nearly impossible to imagine modern astronomy without them<sup>5</sup>. Almost all earthbound observatories and space telescopes are equipped with CCDs. They enable the detection of radiation ranging from the far infrared ( $\lambda \lesssim 300 \mu\text{m}$ ), e.g. the Infrared Space Telescope ISO or the Spitzer Space Telescope) over the optical spectral range to the soft X-ray spectrum (with photon energies of  $E \sim 5 \text{ keV}$ , for example on the x-ray satellites Chandra and XMM-Newton). The widespread use of CCD detectors is due to several fundamental advantages compared to other light detection devices such as the photographic plate (photographic emulsion), photomultipliers, digicons, tv cameras, etc. The main advantages are:

- high sensitivity (high quantum efficiency of up to 90%)
- high dynamical range (16 bit)
- linearity over almost the entire dynamical range
- large spectral range (mid-infrared to ultraviolet for “optical” detectors)
- direct availability for further computer-aided data analysis

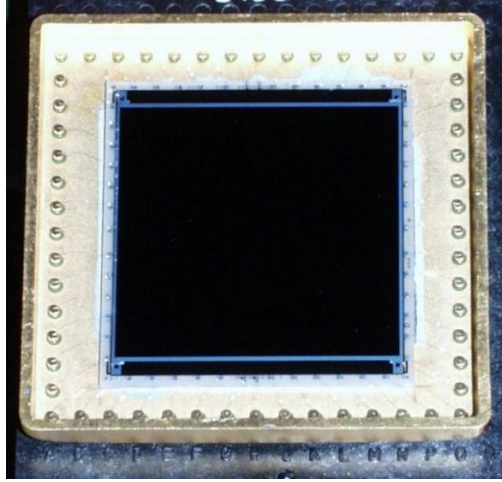
A CCD detector consists of a two-dimensional array of picture elements (pixels), which are light-sensitive metal oxide semiconductor (MOS) capacitors on a silicon substrate. Incident photons excite electrons into the conduction band, after which they get collected in the potential wells of the capacitors. After the integration of

---

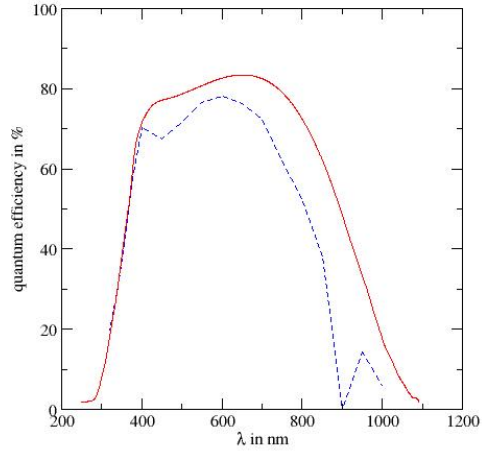
<sup>3</sup>An exception is the radiation coming from our Sun.

<sup>4</sup>In radio astronomy, Jansky (Jy) is a commonly used unit to measure the monochromatic flux.

<sup>5</sup>CCD detectors are now also widely used in the industry, consumer electronics, and many other fields of science.



(a) CCD chip



(b) Quantum efficiency

Figure 1: CCD detector Tektronix TK 1024: (a) Picture of the detector chip. The chip appears black due to its high light absorption. (b) Quantum efficiency curve of the detector as determined by the Observatoire de Haute Provence (OHP, red continuous curve) and the European Southern Observatory (ESO, blue dashed curve). In the wavelength range of 400 to 800 nm the efficiency is about 80%. See section 3 for more details.

light is finished, an alternating voltage is used to shift the collected charge column by column to a readout column. The readout column is finally read out pixel-wise and the resulting signal gets amplified and converted to a digital signal by an analogue digital converter (ADU). Since the first CCD (that was designed as a data storage device by Boyle and Smith at Bell Laboratories in 1970(Boyle & Smith, 1970)), the size of the arrays has constantly grown to current sizes of up to a few thousand times a few thousand picture elements<sup>6</sup>. The chip used in this experiment, a  $1024 \times 1024$  “Tektronics TK1024”, exhibits impressive characteristics concerning read out noise and quantum efficiency. The detector is thus well suited for astronomical measurements, where we deal with low light intensities. The instrument was still in use at the 3.5 m telescope on the Calar Alto Observatory in southern Spain not long ago.

## 2.2 Observations

What does it mean when a detector is characterised as “linear”? Physically, this means that an increase in the measured detector signal is proportional to an increase in the incoming photon flux. In the linear regime, it is possible to directly compare the fluxes of different objects. The intensity of the flux coming from the celestial object is directly proportional to the intensity of the measured signal. When the detector reaches its saturation level, it is no longer possible to derive the

<sup>6</sup>For example, Philips produces a 12 micron  $9216 \times 7186$  pixel CCD.



exact number of photons that reached the detector originally. It is very important to always carefully consider the expected integration times for the observed objects. For weak sources integration times can be very long (up to several hundreds of seconds), whereas for bright stars integration times of only a few seconds can already lead to saturation.

Although the CCD detectors have a large dynamical range it is not always possible to simultaneously assure a good signal to noise ratio for weak objects of interest while not saturating very bright stars. The choice for the exposure time is thus dependent on the scientific goals of the specific observation. A photometric analysis and calibration is only possible if a large number of the objects of interest is not saturated.

For the planning of the observations two artefacts in the detector signal have to be further considered. A non-negligible amount of pixels on the detector is “dead”, i.e. they produce no physically significant signal at all. Additionally, a certain amount of pixels is activated by cosmic rays such as electrons,  $\gamma$ -rays, muons, etc., with several pixels around the impact position of the cosmic ray being saturated or showing high numbers of counts. Whereas the amount and distribution of dead pixels stays the same over time, the number of “cosmics” is dependent on the integration time and their distribution is random. To eliminate both of these artefacts from the final image used for the scientific analysis, several exposures (at least 5) are taken of the science object with the telescope being slightly moved between each exposure. This method is called “dithering” or “jittering”. Due to this offset in every frame and the random nature of the cosmic rays the artefacts will be located at different positions in each exposure. When we subsequently align the frames and determine the median of each pixel we can easily remove these extreme values. This method also has the advantage that it improves the signal to noise ratio without saturating brighter sources.

## 2.3 Data Reduction

The intensity over the detector area is not constant due to small scale variations as well as large scale gradients in the sensitivity. These variations are due to imperfections in the production process of the detector (e.g. “bad” pixels, variations in the doping of the semiconductor, residuals on the surface of the chip) as well as contaminations in the optical path (e.g. dust on lenses or filters). Since we want to compare objects imaged by different areas of the CCD chip, we have to correct for these intensity variations. We do this by taking exposures of a flat background (“flat field”), e.g. a patch of sky without any bright objects (“sky flat”) or a homogeneously illuminated area in the dome (“dome flat”). By dividing our observations with the resulting normalised flat field, it is possible to eliminate the variations in the sensitivity from the science frame. For this correction, we assume that these sensitivity variations are constant over time, at least for the duration of an observation.

To determine the photometric luminosities of the observed objects, the measurements obtained by the instrument have to be calibrated by comparison to stars of

known intensity, so called “standard stars”. Of course it is advantageous if standard stars are directly located within the frames containing the science target, but this cannot always be guaranteed, for example when observing galaxies in fields without stars. Then dedicated special observations of standard stars have to be carried out to determine the calibration factor for the instrumental magnitudes.

### 2.3.1 Bias

The voltage produced by electrons collected in each pixel (and later digitised to “counts”) is artificially superposed during the read-out process in the detector electronics by a small constant positive value. This value, the so called “bias”, must be subtracted again from all CCD-Images in the first step of data reduction. To determine its value, we make images of short integration time without exposing the CCD to light, i.e. the shutter remains closed during the exposures. The measured result is a sum of the bias and the electrons produced thermically, the “dark current”. However, the contribution of the dark current is very small (in order of 0.01 e<sup>-</sup> s<sup>-1</sup> pix<sup>-1</sup>) at operating temperatures of the CCD and thus practically negligible.

### 2.3.2 Flat-field

It is impossible to make the individual pixels of an array absolutely identical. The differing pixel properties cause intrinsic differences in the pixel sensitivities with the consequence that two adjacent pixel areas, illuminated with the same number of photons, will not produce the same number of counts. Moreover, the large-scale illumination pattern caused by the optics (“vignetting”) as well as dust particles on the glass surfaces in the camera (filter, entrance window) will introduce instrument- and time-dependent artefacts on the raw images that must be removed. We can correct for this error by exposing the detector to a surface that shows homogeneous emission over its field of view, which allows us to directly record the variations of the pixel sensitivities. This is called flat-fielding and is a standard empirical method applied in optical astronomy.

## 2.4 Basic principles of photometry

With CCD detectors it is possible to measure the radiation flux reaching the Earth from astronomical objects. Astronomical units are often different from those commonly used in physics. For example, the intensity of a star is given in “magnitudes”. We will now try to clarify the connection between this unit and the physical properties of stars.

The flux  $F$  from a star reaching an observer in a distance  $d$  is given by

$$F = \frac{L}{4\pi d^2} \quad (1)$$

where  $L$  is the luminosity of the star. The SI unit for the luminosity is J/s or W; in astronomy the cgs system is commonly used where the corresponding unit

is erg/s ( $1 \text{ erg/s} = 10^{-7} \text{ J s}^{-1}$ ). However, it can be much more useful to work in units that take our Sun as a standard, since this allows us an easy comparison. This is why in the majority of cases the radiation flux is given in solar luminosities ( $1L_{\odot} = 3.846 \cdot 10^{26} \text{ W}$ ).

The flux of a star is connected to its surface temperature by the Stefan-Boltzmann law:

$$F = \sigma T_{\text{eff}}^4 \quad (2)$$

where  $\sigma = 5.67 \cdot 10^{-8} \text{ W m}^{-2} \text{ K}^{-4}$  is the Stefan-Boltzmann constant. The effective temperature  $T_{\text{eff}}$  is the temperature a black body with the same surface as the star would need to emit the same radiation power. With  $L = A \cdot F = \text{Area} \times \text{Flux}$  it is simple to derive a relation between luminosity and temperature:

$$L = 4\pi R^2 \sigma T_{\text{eff}}^4 \quad (3)$$

where  $R$  is the radius of the star. Taking the example of our Sun with  $R_{\odot} = 6.96 \cdot 10^8 \text{ m}$  and  $L_{\odot}$  given as above this leads to  $T_{\odot, \text{eff}} = 5770 \text{ K}$ .

A further parameter of prime interest is the mass of the star. The mass considerably influences the evolution of the star, with the fate of the star being almost entirely determined by its initial mass<sup>7</sup> Unfortunately, it is not trivial to deduce the mass of a single star from easily accessible observables.

The intensity of the incoming flux from a star, and thus the number of photons detected by a detector, decreases with the square of the distance (see eq. 1). As the distance is in most cases unknown it is not directly possible to specify the luminosity. The problem is aggravated by the circumstance that every instrument exhibits a different sensitivity to the light of the star. Thus it is necessary to introduce different magnitude scales:

The *instrumental magnitude* is a relative unit, allowing the comparison of different sources in one observation, or possibly in different observations with the same instrument and under similar conditions. The measured counts are converted to a logarithmic scale with arbitrary zero point:

$$m_{\text{inst.}} = \text{zero point} - 2.5 \log \text{counts} \quad (4)$$

To accurately determine the total counts a point spread function (PSF) is fitted to the profile of the star or simply all the counts within an aperture centered on the star are summed up (this requires the subtraction of an estimated value for the background offset). With the help of standard stars with known magnitudes the instrumental magnitude can be converted to the apparent magnitude.

The *apparent magnitude* is the brightness of the star as perceived from Earth. The first to introduce an apparent magnitude scale was Hipparch (ca. 150 b.c.).

---

<sup>7</sup>Another important factor for stellar evolution is the star's "metallicity", i.e., its amount of elements other than Hydrogen and Helium.

Hipparch classified the stars by eye in brightness classes ranging from 1 for the brightest stars to 6 for barely visible stars. Later this classification was quantified assuming a logarithmic perception of the brightness by the human eye. Thus, a difference of 5 magnitudes now corresponds to difference in the brightness by a factor of 100. For the flux ratio of two stars this translates to

$$\frac{F_2}{F_1} = 100^{(m_1 - m_2)/5}. \quad (5)$$

The offset between instrumental magnitudes and apparent magnitudes can be determined with the help of standard stars. It is then possible to calibrate the observed magnitudes using this offset. The magnitudes obtained with different instruments and under different circumstances can now be compared to one another as all artefacts of the observation itself should be eliminated.

Finally, the *absolute magnitude* is defined as the apparent magnitude the stars would have if they were a distance of 10 pc away<sup>8</sup>. This distance has been chosen arbitrarily to be able to physically compare stars at different distances, i.e. to have an absolute scale for the brightness of a star. The ratio of the flux reaching us (the apparent magnitude) to the hypothetical flux that would reach us if the star stood at a distance of 10 pc can be calculated. Essentially only the apparent magnitude  $m$  and the absolute magnitude  $M$  feature in the resulting formula:

$$\frac{F(10\text{pc})}{F} = \left( \frac{d}{10\text{pc}} \right)^2 = 100^{(m-M)/5} \quad (7)$$

If we know the distance of the star it is possible to determine its absolute brightness from its measured apparent magnitude  $m$ . However, normally the distance to the star is not known. If in such a case the absolute brightness of the star can be estimated by other means (e.g., the spectral class), then the distance of the star simply is determined by

$$d = 10^{(m-M+5)/5} [\text{pc}]. \quad (8)$$

The expression  $m - M = 5 \log_{10} d [\text{pc}] - 5$  is called the distance modulus. For two stars at the same distance the following relation holds:

$$\frac{F_2}{F_1} = \frac{L_2}{L_1} = 100^{(M_1 - M_2)/5}. \quad (9)$$

---

<sup>8</sup>The distance 1 pc (parsec) is the distance at which one astronomical unit (approximately the mean of the aphelion and the perihelion of the Earth's orbit around the Sun, 1 AU =  $1.496 \cdot 10^{11}$  m), appears under an angle of one arcsecond (1"). For small parallactic angles  $p$  and  $1 \text{ rad} = 2.063 \cdot 10^5''$  the distance is given by

$$d = \frac{1 \text{ AU}}{\tan p} \simeq \frac{1}{p} \text{ AU} = \frac{2.063 \cdot 10^5}{p''} \text{ AU} = \frac{\text{AU}}{p''} = 3.262 \text{ ly} = 3.086 \cdot 10^{16} \text{ m} \quad (6)$$

Thus for known luminosity and absolute magnitude of a reference star, it is possible to determine the luminosity of any other star at the same distance from its absolute magnitude.

For both the apparent and absolute magnitude scales, wavelength-dependent and bolometric magnitudes are distinguished. The *bolometric magnitude*,  $M_{\text{bol}}$ , corresponds to the flux integrated over all wavelengths, from the radio waves to x-rays. In practice it is difficult to determine the bolometric magnitude, as the photon detecting devices only cover certain wavelength ranges. Additionally the atmosphere of the Earth is opaque to large amounts of the spectrum. Hence direct measurements of the bolometric magnitude must be performed by space observatories to avoid absorption of a large part of the incoming photons. Nevertheless, we can use theoretical considerations to estimate the bolometric magnitude from earthbound observations. Alternatively, we can use a wavelength-dependent magnitude,  $M_{\lambda}$ , corresponding only to a part of the luminosity in a certain wavelength range, for example a luminosity in the “blue”.

For a detailed measurement of the spectral intensity of the emitted light we need spectroscopic observations. However, we can obtain a rough spectral information by using well-defined filters, which are only translucent at a certain part of the spectrum. The most commonly used system of broad band filters is the so called Johnson system and modifications of it. The following table gives the four standard filters of the Johnson system in the visible spectral range with central wavelength  $\lambda_0$  and width of the filter  $\delta\lambda$ .

Table 1: Spectral setup of the Johnson filter system.

Filter	$\lambda_0$ [nm]	$\delta\lambda$ [nm]	spectral range
U	365	66	ultraviolet
B	445	94	blue
V	551	88	visual (green)
R	658	138	red
I			infrared

For photometry normally several filters are measured so that it is possible to calculate a distance-independent colour index<sup>9</sup>

$$m_B - m_V = M_B - M_V = B - V. \quad (10)$$

The colour index gives principle information on the spectral properties of the object, e.g. that a star is bluer and thus hotter than another star. Not all filters exactly correspond to the Johnson system and there are various other filter systems in use. A correction for a different transmission behaviour compared to a perfect Johnson filter can be applied during the calibration with standard stars. In a first order approach the calibration of the instrumental magnitude assuming a slightly different transmission curve for the  $B$  filter is calculated according to

<sup>9</sup>In the following equation  $m_V$  often is replaced by the filter name  $V$

$$B = b + b_0 + c_B(b - v) + a_B \cdot \text{airmass} \quad (11)$$

where  $B$  is the apparent magnitude in the Johnson system and  $b$  the measured instrumental magnitude. The zero-point  $b_0$ , the colour correction  $c_B$  and the correction for the airmass  $a_B$  have to be determined by comparison with the standard stars.

## 2.5 The Hertzsprung-Russell-Diagramm

At the beginning of the 20th century, enough stars were photometrically measured to perform statistical analysis on them. It was noticed then, that basic parameters of the stars changed with spectral classification. O stars at the one end of the classification scheme were identified as young, massive and luminous objects, while M stars on the other end were low mass and faint objects. The relation between the spectral type, which is physically connected to the effective temperature  $T_{\text{eff}}$ , and the luminosity is referred to as the Hertzsprung-Russell diagram (HRD). Hertzsprung and Russell independently discovered this correlation at the beginning of the 20th century. The majority of the stars in the diagram is located along the so called main sequence, which is characterised by the hydrogen burning phase during the main phase of a star's life. Other areas in the diagram are populated by stars at different stages during their life. For a stellar population of the same age, as is the case in stellar clusters, the HRD shows the evolutionary history of the population.

In practice, however, it is not simple to compose a HRD, as absolute magnitudes or luminosities and the spectral types of the stars are not well known. This is especially the case for the spectral types: spectra for every object would have to be obtained for their classification. In observational astronomy the colour magnitude diagram (CMD) is used instead. In this diagram the apparent magnitude  $V$  is plotted over the colour index (e.g.  $B - V$ ), which is connected to  $T_{\text{eff}}$ . Both quantities are directly deducible from observations with two filters. The colour magnitude diagram is equally comprehensive as the Hertzsprung-Russell diagram and important conclusions about stellar evolution can be derived from it. In the following sections important methods for the calibration and analysis of such a diagram will be discussed.

### 2.5.1 Shift of the main sequence

Assuming that all stars in a star cluster are approximately at the same distance and have the same chemical composition as well as similar ages, the distance to the cluster can be determined. For this purpose the measured, apparent magnitude is plotted versus the colour, e.g.  $V$  versus  $B - V$ . The position of the main sequence is then compared to the position of a cluster with known distance, assuming that the absolute magnitude of the main sequence is the same for star clusters. Small effects due to different metallicities (see section 2.6) are ignored

here. The assumption is justified for old stellar populations as only low mass stars with uniform development are still located on the main sequence. The main sequence of the observed cluster is shifted in direction of the magnitude axis and aligned with the main sequence of the cluster used for comparison. The amount by which the diagram has to be shifted corresponds directly to the distance modulus of the cluster, neglecting attenuating effects by interstellar dust. The distance of the cluster can now be determined by taking into account the distance of the cluster used for comparison. Alternatively to the comparison with a cluster of known distance, the measured main sequence can also be compared to predictions of its position by theoretical models of stellar evolution. Today, detailed models of the evolution of stellar populations exist. Evolutionary tracks can be calculated, showing the displacement of stars of defined mass in the plane of the colour magnitude diagram during their lifetime. Theoretical curves representing the position of the stars of a stellar population of the same age can be calculated from these curves. The latter curves are called “isochrones”, for example the isochrones denominated Y<sup>2</sup>(Yonsei-Yale) Isochrones (Yi et al., 2003).

Assuming that all stars within the cluster were formed at about the same time, one can also determine the age of the cluster from the colour magnitude diagram: The most massive and luminous stars have a short lifetime and thus only stay on the main sequence for a short period of time (several million years). The reason for this is the mass-dependent luminosity of stars and therefore the mass-dependent time a star spends on the main sequence:

$$L \propto M^a \quad (12)$$

$$\tau_{nuc} \propto \frac{M}{L} = M^{(a-1)}. \quad (13)$$

The exponent  $a$  is mass dependent as well (e.g. 3.5 for  $2M_{\odot} < M < 20M_{\odot}$ ). This means, that first the massive stars at the top left end of the colour magnitude diagram drift into the red giant branch, after all their hydrogen has been burned in their cores. With increasing age of the stellar population lower mass stars also start moving into the red giant branch. This shifts the so called *turn-off point* in the diagram to lower masses and luminosities. From the position of the turn-off point it is hence possible to determine the age of the cluster. For old clusters this method allows a good determination of the age, for young clusters caution is advised, as often no unambiguous turn-off point can be defined. The position of the turn-off point is also dependent on the metallicity of the cluster, which has to be considered when doing the comparisons.

## 2.6 Stellar clusters

Stellar clusters can be roughly divided into two groups: Open clusters and globular clusters (GC). The main difference between the groups are the age and the mass of the clusters. Globular clusters are much older and more massive than open clusters. GCs are among the oldest objects found in the universe. Occasionally,

they even seem to be older than the universe itself! However, the ages of GCs have large errors and comparisons between different measurements can show large discrepancies. The stars in globular clusters of our Galaxy are very metal poor, they consist almost only of hydrogen and helium (which is approximately the composition of the matter found in the universe after the big bang) with only minor contaminations by higher elements, i.e. metals. The deficiency in metals is an indication that these objects must have formed in the very early phases of the universe when the interstellar matter was not yet enriched with heavier elements. Stars with such a metal deficiency are classified as population II stars.

Globular clusters are spherically symmetric objects, dispersed all over the Milky Way halo with a slight concentration towards the centre. They constitute a major portion of the halo of our Galaxy up to radii of 55 kpc from the galactic centre. In total about 150 globular clusters are known to orbit our Milky Way. It is assumed that the majority of GCs formed at the beginning of the evolution of our Galaxy. Thus their distribution, velocity and composition give information about the evolution of the Milky Way.

Open clusters on the other hand have a wider range of ages between a few Myr up to a few Gyr. The metallicity of open clusters varies as well depending mostly on the age and the location within the host galaxy of the open cluster. Therefore open clusters are good tracers for the evolution of galaxies, as many properties (age, metallicity, etc.) of their stars are more easily determined than for isolated field stars. Open clusters are also very good tracers of star formation, since most stars are formed in clusters.

Most of the open clusters of the Milky Way are located within the disc of our Galaxy. There are about 1000 open clusters known within the Milky Way. However, their total number is likely much higher, since their lower surface brightness means that we are not able to detect them to such a great distance as the more compact GCs and many open clusters are hidden behind dust clouds and the Galactic center.

As all stars of a stellar cluster are located at about the same distance and have the same metallicity and age<sup>10</sup> they are especially well-suited for the analysis with a Hertzsprung-Russell diagram. The colour magnitude diagram of the star cluster Messier 92 (M92) has a characteristic form as can be seen in figure 2. Stars in different evolutionary phases such as main sequence stars (hydrogen burning phase) and giants (helium burning phase) can be located easily.

---

<sup>10</sup>There are however globular clusters for which two red giant branches are found indicating a second generation of stars ((Milone et al., 2008)).



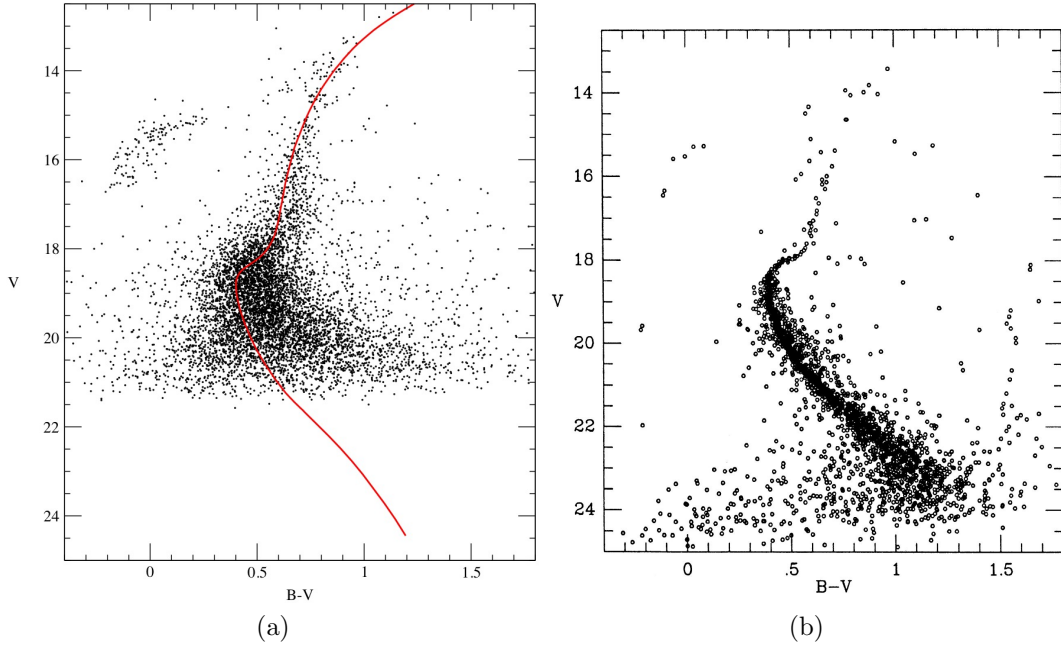


Figure 2: Colour magnitude diagram of the bright globular cluster M92: (a) Colour magnitude diagram from data observed with the 70 cm telescope of the MPIA on 07/06/2004 by K. Tristram. A  $Y^2$  isochrone for a metallicity of  $[\text{Fe}/\text{H}] = -1.9$ , an age of 16 Gyr and a distance modulus  $\Delta = 14.8$  mag is plotted into the diagram. (b) Diagram published in 1988 by (Stetson & Harris, 1988). The observations of Stetson and Harris go four magnitudes deeper than the observations with the 70 cm telescope.

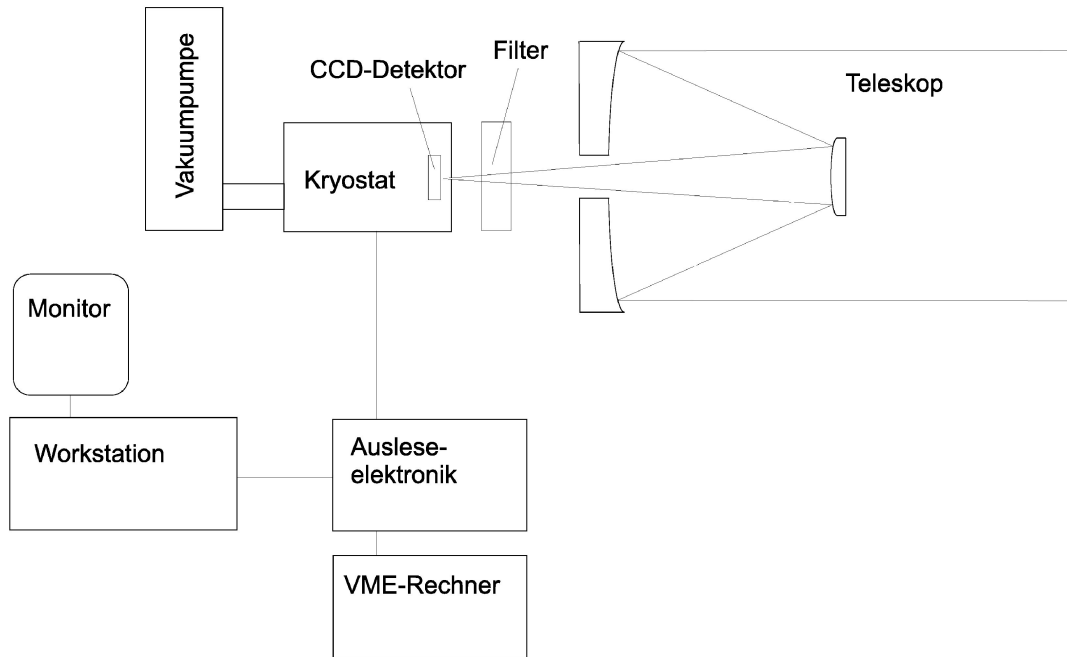


Figure 3: Diagram of the instrumental setup as of January 2006.

### 3 Layout of the experiment

The setup of the experiment is given by the sketch in figure 3. Light gathered by the primary mirror is imaged on the CCD-detector, which is cooled with liquid nitrogen within an evacuated cryostat. To read out the detector, a pulse generator, amplifier, and analogue-digital-converter is needed, which are put into a separate box, mounted on the telescope itself. A graphical user interface allows easy use of the camera and access to the data and can be started from the available workstation. As with every astronomical instrument in use, continuous changes and improvements are performed to increase the ease of use and the availability of the data.

#### 3.1 Hardware

The experiment is performed with the 70 cm telescope at the Max-Planck-Institut für Astronomie (MPIA) on the Königstuhl mountain. The telescope is depicted in figure 4, the general setup can be seen in figure 3. The telescope structure was built at the institute in order to have a facility to test cameras and other astronomical devices built at the MPIA. Therefore it has a parallactic mounting. This enables to switch between two different foci: Cassegrain mode - which is used in our experiment - and Coudé focus, which decouples the beam through the polar axis and enables to attach large instruments on the ground floor, where the beam ends. In the past, another reason for this kind of mounting was the easy compensation of Earth's rotation by just rotating around the polar axis.

After reflection by the main mirror with a diameter of 70 cm the light is reflected another time by the secondary mirror and reaches the camera (for the Cassegrain case) through a hole in the primary mirror. The position of the secondary mirror can be changed to adjust the focus of the telescope (by pressing the respective button on the control panel). The camera used for this experiment is located in the Cassegrain focus below the main mirror in a cryostat cooled by liquid nitrogen (see figure 4). Before cooling the camera with liquid nitrogen the dewar has to be evacuated to a pressure of about  $p = 10^{-6}$  mbar to suppress heat conduction and avoid water vapour to freeze out on the camera and detector. This is achieved by a dual stage vacuum system with a rotary vane pump for the preliminary vacuum and a turbo molecular pump for the high-vacuum. Just above the camera a slider containing up to five filters is located. Usually they are ordered by wavelength, but before using them it has to be checked which filters are installed in the slider. With the help of the camera optics the light gathered by the telescope is focussed on the CCD detector.

The detector is a *Loral/Lessern2k2eb BI* thinned, back illuminated CCD with  $2048 \times 2048$  picture elements and a pixel size of 15 microns. CCD-cameras in general are characterised by a very high quantum efficiency of up to 90%, which makes them ideal for astronomical observations. This explains their widespread use in all observatories over the world. The pixel scale of our camera is  $0.55''/\text{pixel}$  corresponding to an optimal adaption for the seeing conditions on the Königstuhl mountain. Atmospheric turbulences smear out the ideally point-like stellar sources to a profile similar to a Gaussian with a full width half maximum of  $2''$  to  $3''$ . The pixels saturate at a level of 60000 electrons at a gain value of 5.

The box on one side of the telescope contains the readout electronics. It contains a pulse generator for the read-out procedure, an amplifier, analogue digital converter as well as the controller for the heater of the CCD-camera (in order to keep it at the ideal temperature of 115 K. The read-out electronics are controlled by a UNIX workstation called “*clearsky*”, as of January 2006 a SunUltra 1 running the operating system Solaris 9 (BSD UNIX).

So far it is not possible to control the telescope position from the workstation, although this feature is planned to be implemented in the near future. The controls are located in a special console in the telescope dome. During the experiment you will only need the controls for declination, right ascension, guiding, mirror protection, and the focus. The observed data is stored via network-attached storage (NAS) on a Linux computer. This computer can also be used for data visualisation and analysis during the experiment and the final data reduction and analysis. The Dome can be handled via a remote control by pressing at the same time the red button and another functional button for rotating left/right or opening/closing the slit.

## 3.2 Software

This section gives an overview of the software used throughout the experiment and data analysis. Details on the needed commands are given in the respective sections,

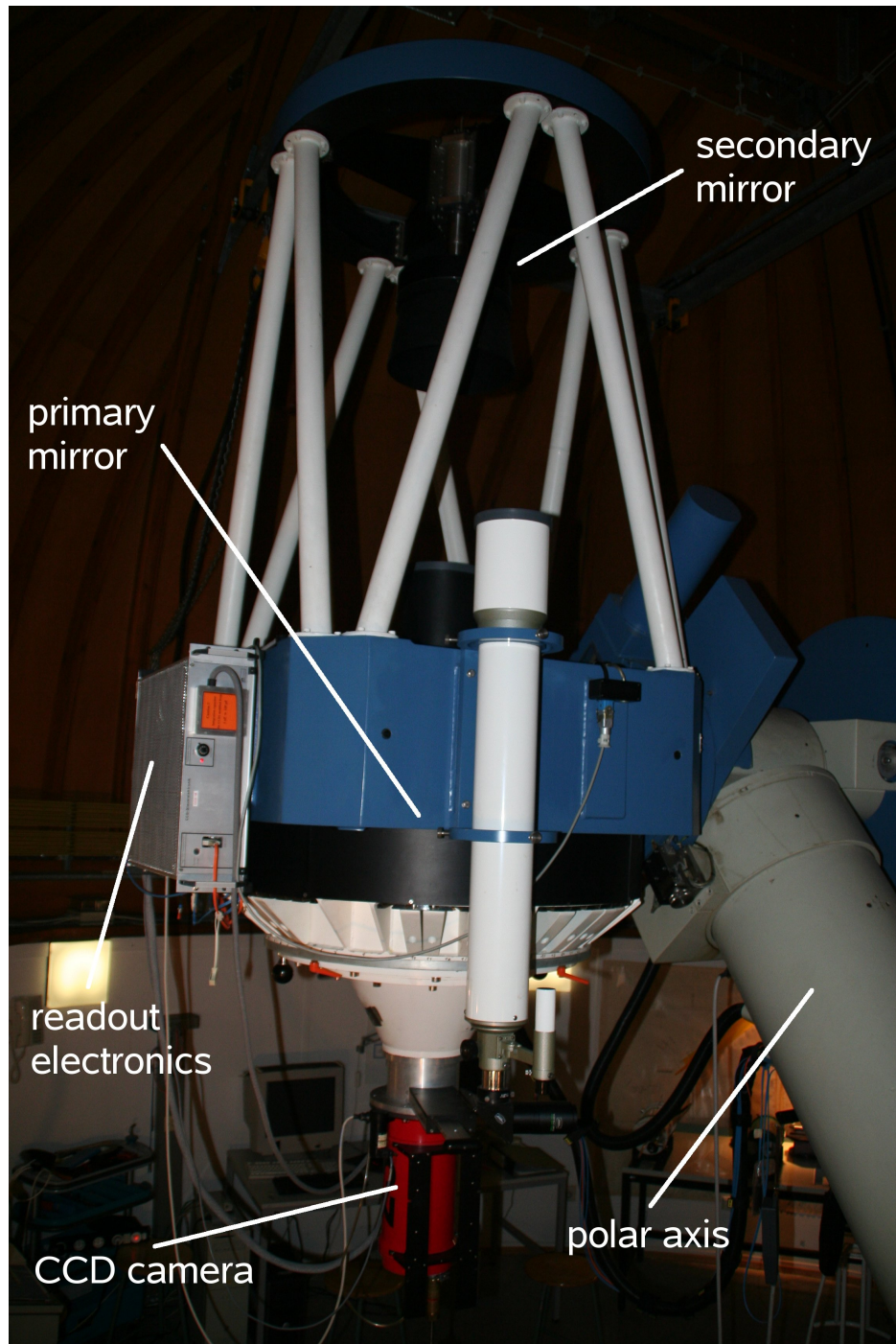


Figure 4: The 0.7 m KING (Königstuhl Instrument for Night-sky Gazing) telescope at the MPIA. The major components of the telescope are indicated in the picture. The CCD-camera is attached below the main mirror in the Cassegrain focus. It is situated in the red cylindrical dewar, which is cooled with liquid nitrogen. Also visible is the parallactic mounting of the telescope.

where they are used. The CCD camera is controlled via command line commands on the *clearsky* computer (see section 8 for details). The data reduction, analysis, and part of the visualisation is done with the help of IRAF<sup>11</sup>, which is a standard data reduction package used in astronomy.

Images are displayed with the viewer SAOIMAGE DS9, which can be directly controlled via IRAF commands. For the final data analysis, any plotting/fitting tool (e.g. Python/Matplotlib, Origin, GNU-plot, XMGRACE, etc., or even Microsoft Excel) can be used.

### 3.2.1 IRAF

IRAF is a general purpose software system for the reduction and analysis of astronomical data, which includes a large amount of routines for image processing and graphics. This section gives an overview about some basic procedures and how data visualisation and reduction is handled in IRAF. All commands needed for the reduction procedure and analysis of the data will be given at the corresponding position in this description.

To start IRAF in the home directory, type

```
> cd ~ > cl
```

from within the home directory (actually the directory where the file *login.cl* is located). A new terminal should pop up (in fact a **xgterm**) and a program used for displaying the images (SAOImage DS9<sup>12</sup>) is opened. IRAF is not a very user friendly program and the user has to get accustomed to its peculiarities. In IRAF the commands for image manipulation and visualisation are principally given in command line. A few tasks make use of graphics display (plots, graphs, etc.) and the image display (SAOImage DS9). Some of the tasks, however, also have a so-called graphics or image cursor allowing direct interaction with a graph or image. For example the task **display** can be used to visualise an image in the display window of DS9:

```
cl> display
image to be displayed:  myimage.fits
frame to be written into(1:16) (1):  1
```

The extension *.fits* in the filename can be omitted. The task **imexamine** can now be used to analyse this image and upon invoking this task, an image cursor appears. By pressing “**r**” a radial profile is plotted in the graphics window. Every task in IRAF has a certain set of parameters; some of the parameters have to be specified every time the task is called, others are optional, i.e. hidden. All parameters belonging to a task can be edited with the task **eparam** (e.g. **eparam display**), when finished with editing press “**:q**”. Parameters necessary for the execution of the task are queried, as shown for **display** above. Alternatively, all the parameters can be directly given in the command line, also the optional or hidden ones:

---

<sup>11</sup>**I**mage **R**eduction and **A**nalysis **F**acility; See also <http://iraf.noao.edu/> for detailed information on the software package

<sup>12</sup>For more information on this tool see <http://hea-www.harvard.edu/RD/ds9/>.

```
cl> display myimage.fits 1 ztrans=log
```

Here `ztrans` is a hidden parameter specifying the colour mapping for the image display.

### 3.2.1.1 General IRAF commands

#### 1. Recall commands

Command lines, which have been recently used can be recalled by simply typing

```
cl> e
```

and selecting the wanted command with the arrow keys.

#### 2. Getting help information

```
cl> help command
```

displays information on individual commands, including all options and package dependencies.

#### 3. Looking for packages/commands

```
cl> apropos taskname
```

Gives a summary of all expressions linked to “taskname”; can for example be used to figure out which program packages have to be loaded (by simply typing their names) in order to get access to a certain command.

#### 4. Changing command options

Parameters of commands can either be changed directly on the command line or within the parameter menu, which can be opened by typing

```
cl> epar command
```

This is short for *edit parameters*. Within the menu, parameters are changed by simply overwriting them. Some parameters contain sub-menus, which can be entered by typing “:e” (this should remind you of the text editor *vi*).

#### 5. Displaying images

As explained above, images are displayed with the image viewer DS9, which can be controlled from within IRAF. To open an image type:

```
cl> disp image frame
```

where `image` is the fits-image (the suffix `.fits` can be omitted) and `frame` is the number of the frame where it should be read into (several images can be opened at the same time in different frames).

## 6. Simple analysis of images

A simple way of taking a first glimpse at the data can be done with the help of

```
cl> imexam
```

The mouse then turns into a graphics cursor and different operations can be executed by pointing to a certain area on the image and pressing

- r plots radial profile (within some pixels) in a separate graphics window
- s draws a surface plot (within some pixels) in a separate graphics window
- a does a simple aperture photometry and prints the results at the prompt
- m some statistics within some pixels around the location of the graphics cursor printed at the prompt

## 7. Command Abbreviation

All IRAF-commands can be abbreviated as long as they remain unambiguous, e.g. `lo` instead of `logout`.

### 3.2.1.2 IRAF commands for data analysis and extraction

#### 1. Extract information from FITS headers

Any keyword of a FITS header can be extracted with the following command:

```
vocl> hselect file.fits KEYWORD yes
```

For extracting the keyword from multiple files, e.g. *file0001.fits*, *file0002.fits*, etc., use `file*.fits`

#### 2. Create a list of file names

To create a list containing the file names *file0001.fits*, *file0002.fits*, etc. use the command

```
vocl> files file*.fits > listfilenames.txt
```

Be aware that this command will not overwrite files, so there cannot already be a text file with that name.

You can check the contents of the list file with the `type` command, e.g.:

```
vocl> type listfilenames.txt
```

#### 3. Performing simple arithmetic operations

Simple arithmetic operations (e.g., `+`, `-`, `/`) can be performed with the `imarith` command, e.g.

```
vocl> imarith file1.fits / value file1_new.fits
```

divides all data values of *file1.fits* by *value* and saves the result in a new fits file called *file1\_new.fits*.

*imarith* can also deal with lists, e.g.

```
vocl> imarith @list1.txt - @list2.txt @list3.txt
```

subtracts the values of *list2* from *list1* (row by row) and saves the results in *list3* (the @ in front of the list name tells IRAF that this is a list). This only works if *list1* and *list2* have the same number of rows and one column each. Additionally, any header information in the lists (rows starting with #) have to be deleted first. To subtract one fixed value for all entries of *list1* simply replace *@list2.txt* by *value*, e.g. the median.

#### 4. Combine FITS images

FITS images can be combined with the command *imcombine*, e.g.

```
vocl> imcombine @listfilenames.txt filename.fits combine=median
```

determines the median values of all the files listed in *listfilenames.txt* and saves it as a new FITS file called *filename.fits*.

#### 5. Extract statistical information

Statistical information can be extracted from a FITS image with the *imstat* command, e.g.

```
vocl> imstat file*.fits[10:1000,20:900] fields='midpt' > list.txt
```

calculates the median value of the pixels in the range  $10 \leq X \leq 1000$ ,  $20 \leq Y \leq 900$  for the files *file0001.fits*, *file0002.fits*, etc., and saves it in the list *list.txt*. To get the standard deviation instead use *fields='stddev'*.

#### 6. Extract histogram values

Histogram values can be extracted with the command *imhistogram*, e.g.

```
vocl> imhistogram filename.fits listout=yes > histogram.txt
```

extracts the histogram values from *filename.fits* and saves it in the list *histogram.txt*.

### 3.2.2 SAO-Image DS9

The best way to get an idea of how SAO-Image DS9 works is to open an image and to play around with it. Most of the menu structure and buttons should be



self-explanatory. We would like to give just a few hints, which might be useful for our image analysis:

1. For most of our data-sets, a reasonable representation can be obtained by pressing the buttons *Scale*  $\rightarrow$  *zscale*
2. Push the right mouse button while moving over the image. This will change the color-scale as well.
3. The color-scale can be reset via the menu *Color*  $\rightarrow$  *Reset Colormap*
4. In order to take a look at the differences between two images, load them in two different frames. Comparison by eye can easily be done by pushing *Frame*  $\rightarrow$  *prev/next*.

As for all scientific equipment also the setup of this instrument is constantly being improved. Changes in the hardware and software are planned for the near future, e.g., the controlling of the telescope from the workstation. The layout as described above should hence not be considered final.

You should also keep in mind that you are dealing with expensive equipment, which is also in use by other people of our institute to obtain and handle scientific data, so please be cautious. However, you are encouraged to bring in and follow your own ideas (in coordination with your supervisor).

## 4 Characterization of the CCD

### 4.1 Preparations

Before any scientific observations can be carried out with a CCD camera it has to be cooled down with liquid nitrogen.

*What is the reason for the cooling?* (Keep in mind that a CCD is a silicon-based semi-conductor.)

To allow the cooling of the dewar (the "can" containing the CCD chip), it has to be evacuated with a vacuum pump. This is normally already done by the supervisor. After arrival at the telescope you will have to power down the pumps, close all valves and detach the pumping station from the telescope to allow the telescope to be moved.

In the next step, the instrumentation has to be switched on from the console for the telescope controls. Now the electronics which can be controlled via a Linux PC are able to "talk" to the CCD and images can in principle be taken. Before that, however, the readout electronics have to be reset and newly initialized. This is also done from a terminal on the Linux PC *clearsky* via the following command:

```
> ccdread -R -I -C 1
```

The parameters mean the following: -R tells the electronics to reset the CCD, -I to re-initialize it and -C 1 short-circuits the pixels so that they are "empty".

You should now change to your private data directory using the terminal command `cd` (create directory with `mkdir`), where it is possible to make a first exposure with the camera:

```
> cd data/name_of_group
> ccdread -C 0 -f test.fits -E 5.0 -O -C 1
```

The last command tells the CCD to make an image. -C 0 tells the CCD that an image will be taken, -f is followed by the filename (in this case `test.fits`), -E is followed by the exposure time in seconds (here 5.0 seconds) and -O reads out the CCD. It is important to note that at this stage the detector still has ambient temperature and the coverage of the primary mirror is normally still closed. That means that most of the signal we would see on the image are charged particles that were produced mainly thermally<sup>13</sup>. To visualise the image, the program `ds9` is used.

```
> ds9 &
```

The ampersand (&) allows running a program in the background, so that it does not block the terminal window. In `ds9`, colour mapping can be changed using the right mouse button.

The image shows a strong gradient in read-out direction as those parts that are read out later show a stronger dark current signal. On one side of the image the so called **overscan region** can be seen. This region is not a physical part of

---

<sup>13</sup>cosmic rays might leave also some traces

the CCD chip but is added electronically to the image. These pixels contain no image information but only the positive offset (**bias**) applied to all detector pixels. This offset is required as the analog-digital-converter can only handle positive pixel values and due to fluctuations or bad behaving pixels negative values might otherwise occur. In any case, the bias signal has to be subtracted from all data obtained with the camera in the so-called **bias correction**!

The image can be analysed with the iraf command imexam:

```
> cd ~
> iraf
vocl> cd path/to/your/directory
vocl> imexam
```

On the image display pressing **m** gives statistics on pixels around the cursor position, **s** plots a surface plot, **c** plots a column, **l** a line and so on. Play a little bit around with the first test image and get an idea how the signal varies over the detector and check also the values in the overscan region.

## 4.2 Properties of the dark current

It was already mentioned above that charges that were thermally excited due to the “heat” of the surrounding environment can cause a signal on the CCD. In this section you will learn how to cool a CCD and how the band gap of the semi-conducting CCD material can be derived.

### 4.2.1 Theoretical background

The theoretical dependency of the dark current  $I$  from the temperature  $T$  can be derived from Fermi statistics and has the following form:

$$I = \text{const.} \cdot T^{\frac{3}{2}} e^{-\frac{E_g}{2k_B T}} \quad (14)$$

where  $k_B = 8.617 \cdot 10^{-5} \frac{\text{eV}}{\text{K}}$  is the Boltzmann constant and  $E_g$  the band gap of the semiconductor. Measuring the dark current as a dependency of the temperature enables the determination of the band gap of the semiconductor material of the detector and thus the determination of this important characteristic of the instrumental setup. Apart from the decrease of the dynamical range of the detector by the additionally freed charge, the dark current also deteriorates the sensitivity of the system by its stochastic nature (thermal noise).

To reduce the dark current to negligible levels, CCD detectors are cooled. It is possible to suppress the thermal excitation of electrons to less than 0.01 electrons per pixel and second. For astronomical detectors in the optical wavelength range liquid nitrogen, at a temperature of approximately  $-196^\circ\text{C}$ , is used for cooling. Chips used for observations in the infrared have to be cooled by liquid helium because of the smaller band gaps in these devices. To avoid a deterioration of the

semiconductor properties at very low temperatures the chip used in this instrument is heated to an optimal operating temperature of roughly  $-100^{\circ}\text{C}$ . For short exposure times and high luminosities, for example in digital cameras, no cooling at all has to be applied.

#### 4.2.2 Execution of the measurements

The cryostat should be evacuated before it is cooled. The dewar is filled from the nitrogen container by inserting the rod into the dewar from below. If necessary, nitrogen has to be obtained at the large tank outside the main building and transported into the telescope building in the container. **When handling the nitrogen, glasses and gloves have to be used to avoid serious burning!** Don't worry: Your supervisor will guide you through the cooling process.

Once the dewar is filled with nitrogen you can start measuring the dark current.

*What is actually a good measure for the dark current of a CCD with  $2048 \times 2048$  pixel?* (Keep in mind that all pixels are probably slightly different and some might not be working at all.)

As the CCD is getting cooler and cooler you should read out the chip multiple times to ensure a good sampling of the curve (for this repetitive job it is advantageous if you have a basic knowledge in scripting). The command you need is:

```
> ccdread -C 0 -b 2 -g 5 -T -F dark -E 30 -o dark_current
      -u "name1 name2" -O -C 1
```

The parameters here are: -b 2 leads to a binning factor of 2, meaning that 4 pixels (2 in each direction) will be regarded as one, -g 5 prescribes a gain factor of 5 (equivalent to a certain amplification of the signal), -T saves the current temperature of the CCD, -F is followed by the basis of the filename (a running number will be automatically added), -o gives the possibility to provide a name for the object that is observed and -u lets you specify the observer's names. While the image data is stored in the image part of the .fits-file all the other information is saved into the so-called .fits-header (you can think of it as a "label" for the image). Ask your supervisor, as this step can be easily automated using common programming languages.

#### 4.2.3 Analysis

1. Use IRAF to extract the temperature information from the headers of the FITS files of all dark measurements.
2. Use the IRAF command `imstat` to create a list of median bias values and the standard deviations in the overscan region for all dark measurements (check one of the FITS files with `ds9` to get the range in pixel values of the overscan region).
3. Correct each of the dark measurements with their corresponding median bias value and save these corrected FITS files under a new name (Tip: first use IRAF to create a list of the filenames before the bias correction. Copy this

list and change the file names to indicate that these are the bias-corrected files (e.g., by adding `_b` to the FITS file names.) Then use these lists together with the list of median bias values in the `imarith` task. **Don't forget to always subtract the bias from all of your measurements!**

4. Extract the median dark current values of the **bias-subtracted** FITS files of the dark measurements with the IRAF task `imstat` (use `ds9` again to get the proper range in pixel values of the image region of the CCD).

#### 4.2.4 Tasks and discussion points for the protocol

- Verify the dependency according to eq. 14 by plotting the data and the theoretical curve in a sensible plot (see Figure 5).
- Determine the band gap of the detector chip by fitting the dependency.
- Determine the bias and its scatter for two images, one at the beginning of the experiment and one at the end.
- Why do we have to determine and subtract the bias value for every image individually?
- Discuss reasons for possible deviations from the expected band gap value.

### 4.3 Flat-field correction

Both small scale (different sensitivity of single pixels) as well as large scale variations (dust, optical effects) have an influence on the detector signal and thus on the resulting image. To correct for these effects every (scientific) raw frame has to be divided by a so-called master flat-field, which is an image of a structureless, well illuminated (white) surface. By combining several individual images we neglect artefacts on single frames and also reduce the noise. **This correction has to be done for every filter that will be used for the scientific observations** as it accounts for small imperfections (e.g., dust) in the optics.

#### 4.3.1 Execution of the measurements

To obtain flatfields, point the telescope to the white surface hanging on the inner side of the dome by pressing the RA and DEC buttons on the control console. Make sure that the cover for the primary and secondary mirror are open and take a first test flat-field image with the command:

```
> ccdread -C 0 -b 2 -g 5 -T -F flat -e 30 -o "flat_filter_"  
      -u "name1 name2" -O -C 1
```

While before we had an upper case `-E` followed by the integration time in seconds we now have to type a lower case `-e` followed by the integration time. The difference is that with `-E` the shutter within the camera is not opened (good for taking dark

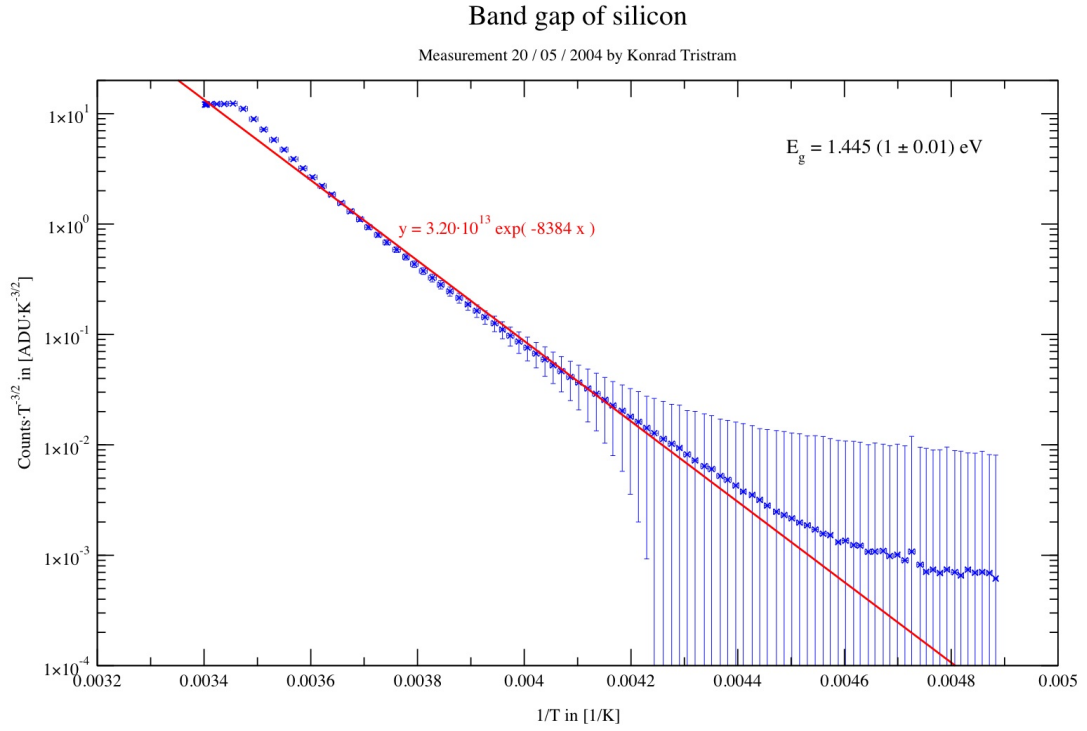


Figure 5: Determination of the band gap  $E_g$  for the detector according to formula 14. To better see the deviation of the measured signal from the theoretical behaviour the dependency has been transformed into a linear dependency. The band gap of this measurement determined by Konrad Tristram on 20/05/2004,  $E_g = 1.445 (1 \pm 0.01) \text{ eV}$ , is considerably higher than the band gap of silicon,  $E_{g,\text{SI}} = 1.15 \text{ eV}$ .

frames) while the `-e` opens the shutter and photons can be detected. To obtain a sensible signal at longer integration times the illumination inside the dome has to be dimmed. You should test the optimal setting for each filter before starting the measurement. To obtain a master flatfield frame, take at least five exposures at relatively long integration times to achieve a good signal to noise ratio for each filter. However, the maximum pixel value across the array should still lie well within the region of linearity.

### 4.3.2 Analysis

1. Use IRAF to subtract the bias from the individual flat-field images similar to the dark current correction in the previous section (use the `imstat` and `imarith` commands).
2. Combine the individual flat-field images to a single image (the master flat-field) with the IRAF task `imcombine`. (Tip: Use IRAF to write all file names first into a list and use this list in `imcombine`. Take the median of the images.)
3. Use the IRAF task `imarith` to normalize the master flat-field to one by dividing it by its median.
4. Use the `imhistogram` command in IRAF to obtain a histogram for this master flatfield.

### 4.3.3 Tasks and discussion points for the protocol

- Perform a flat-field correction for one of the single flat-field images (i.e., divide the image by the normalized master flat-field). Plot and compare the image before and after the flat-field correction. (Tip: The FITS images can be saved in ds9 as image files, e.g., in the JPG or PS format.)
- Plot and discuss the histogram for the normalized master flat-field.
- Why do we have to normalize the master flat-field?
- How many pixels of the master flatfield have a value close to 1 as expected and where do the deviations come from?
- Why do we need to divide all of our observations by a master flat-field?
- Why do we use the median of the pixels for the image combination and for the normalization and not, for example, the mean value?
- Why was it necessary to set the illumination differently for each filter?
- Why do we have to measure the CCD response to a "flat" surface? Why are the nails holding the blanket and the warped surface of the blanket itself not detrimental to the dome flat?

## 4.4 Linearity and dynamical range of the CCD

To quantify the sensitivity to incoming photons and the limitations of the chip the linearity and dynamical range have to be analysed. For this, we measure the detector signal for flat-field images for different illuminations (in this case for different exposure times) in the R filter. The filters can be changed with the movable filter-frame located above the CCD dewar.

### 4.4.1 Execution of the measurements

The setup is similar to the one for the master flat field (section 4.3.1), but now we take exposures of the uniformly illuminated area with different integration times. The collected charge and hence the signal should be proportional to the integration time, assuming the illumination is proportional to the integration time. In total, you should take about 15 images with increasing exposure time, of which the last 2-3 should already be in the saturated area.

### 4.4.2 Analysis

1. Use IRAF to subtract the bias from the images similar to the dark current correction in the previous section (use the `imstat` and `imarith` commands).
2. Use the IRAF command `imarith` to perform a flat-field correction for all images by dividing them by the normalized master-flat from the previous section.
3. Use the IRAF task `hselect` to extract the exposure time information from the headers of the FITS files.
4. Use the IRAF command `imstat` to get the values for the median and the standard deviation for all the bias- and flat-field-corrected images.
5. Repeat the above steps for the I-filter images obtained in the next section of the lab. Note that those images were obtained in the next section and are therefore in the 'sensitivity' folder. Clearly, you should do this task using one image in each pair taken.

### 4.4.3 Tasks and discussion points for the protocol

- Verify the linearity and the dynamical range of the chip and determine the linear regime (for both filters) by plotting the signal of each flat-field image against its integration time.
- Determine the deviation from a perfect linear relationship and specify the intensity where saturation sets in (see Figure 6). Use only those frames that are not saturated for the fit. Estimate the error of the measurement from the standard deviation of the pixel values.



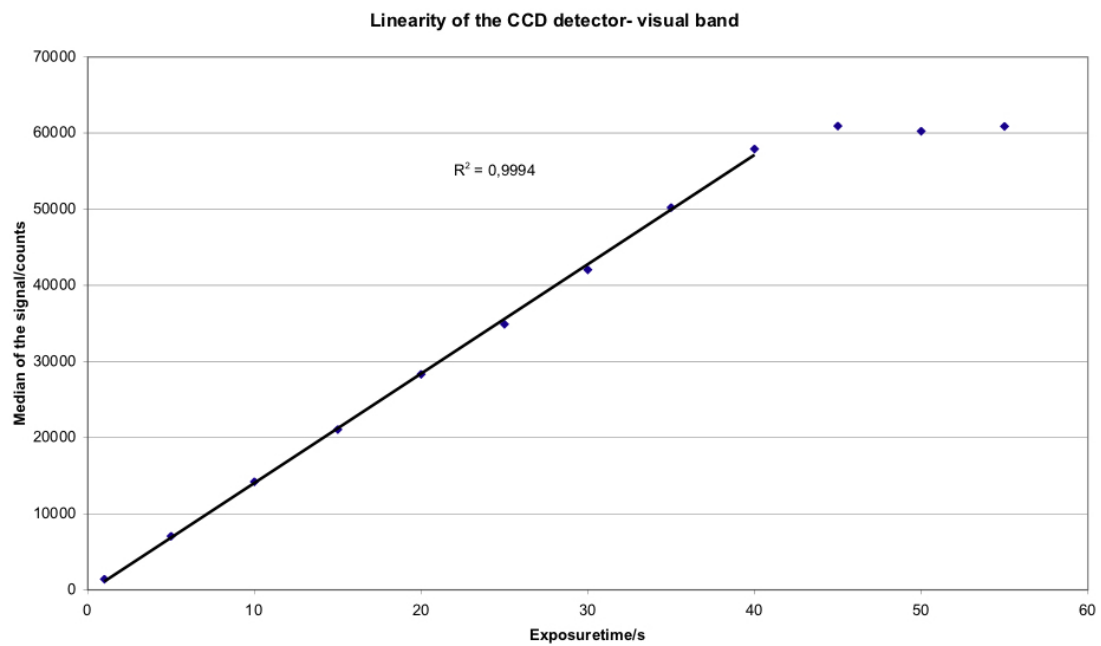


Figure 6: Linearity and dynamical range of the detector. The illumination is assumed to be proportional to the integration time. The plot shows that the detector signal is proportional to the integration time (and hence the illumination) with less than 0.5 % deviation. The detector saturates at approximately 60000 counts for a gain factor of 5.

## 4.5 Sensitivity of the detector and noise properties

According to Poisson statistics, the variance of the pixel-to-pixel fluctuations in a uniformly illuminated area scales with the number of incoming electrons per pixel,  $N_e$ , such that

$$\sigma_e^2 = N_e \quad (15)$$

For astronomical data reduction, the gain,  $\kappa$ , that is the number of excited electrons per unit of the analogue digital converter (ADU), is an important characteristic of the system. It is a required parameter in signal processing. The final signal  $N_{e,d}$  in ADU is connected to the original number of incoming photons  $N_e$  by

$$N_e = \frac{\kappa}{\eta} N_{e,d} \quad , \quad (16)$$

where  $\eta$  is the quantum efficiency of the detector. Similarly,

$$\sigma_e^2 = \frac{\kappa^2}{\eta^2} \sigma_{e,d}^2 \quad . \quad (17)$$

Using the above relations, we get

$$\frac{\kappa}{\eta} N_{e,d} = \frac{\kappa^2}{\eta^2} \sigma_{e,d}^2 \quad , \quad (18)$$

so that,

$$\sigma_{e,d}^2 = \frac{\eta}{\kappa} N_{e,d} \quad . \quad (19)$$

Two other sources of noise exist in the data aside from the photon noise. The read-out noise of the gate amplifier,  $\sigma_R$ , and the so-called Pixel Response Non-Uniformity (PRNU) noise,  $\sigma_{PRNU}$ , which occurs due to the fact that the quantum efficiency of the pixels are not exactly identical. The PRNU noise increases linearly with signal level such that

$$\sigma_{PRNU,e} = N_e f_{PRNU}, \quad (20)$$

where  $f_{PRNU}$  is the detector-dependent, characteristic PRNU factor, which is typically on the order of 0.01. Therefore, for this typical value, the photon noise and PRNU noise are exactly the same at a signal level of 10 000 electrons, ( $\sigma_{PRNU,e} = 0.01 \cdot 10\,000 = \sigma_e$ ), and PRNU noise dominates at high signal levels. The total noise of the measured signal in ADU is given by

$$\sigma_{tot,d}^2 = \sigma_{e,d}^2 + \sigma_{R,d}^2 + \sigma_{PRNU,d}^2 \quad . \quad (21)$$

Since the underlying cause of PRNU noise is a physical one and directly proportional to the signal level, two frames with the same signal level should have the same PRNU noise. Therefore, by subtracting the two flat frames with the same signal level, one eliminates the effect of PRNU all together. The only source of

noise left in this difference image,  $\sigma_{\text{diff}}$ , is then a combination of read-out noise and photon noise, such that after propagating the errors,

$$\sigma_{\text{diff},d} = \sqrt{2} \cdot \sqrt{\sigma_{R,d}^2 + \sigma_{e,d}^2} \quad . \quad (22)$$

Combining eqs. (19) and (22), and assuming  $\eta = 1$ , one can derive

$$\sigma_{\text{diff},d}^2 = 2 \left( \sigma_{R,d}^2 + \frac{N_{e,d}}{\kappa} \right) \quad . \quad (23)$$

#### 4.5.1 Execution of the measurements

The setup is similar to the one for the linearity measurements (section 4.4.1), but now we take two measurements of the uniformly illuminated area with the same integration time for a range of exposure times in order to remove the effect of PRNU. In total, you should take about **20 pairs of images with increasing exposure time in the I-filter**, of which the last 2-3 should already be in the saturated area.

#### 4.5.2 Analysis

1. **For one pair of images** where on average the signal does not exceed  $\sim 30\,000$  counts. Determine the read-out noise,  $\sigma_{R,d}$ , from the overscan region by using the IRAF routine `imstat`.
2. Use ds9 to choose at least a  $200 \times 200$  pixel region that is uniformly illuminated near the center of the image. *It is important to choose a uniformly illuminated area because in the following steps we are working with the raw images and will not be performing any bias-subtraction or flat-field corrections!*
3. Using the IRAF routine `imstat`, determine the total noise,  $\sigma_{\text{tot},d}$ , and the median signal,  $N_{e,d}$ , in each of these two images within the chosen regions.
4. Using the IRAF routine `imarith`, subtract the signal of one image from the other.
5. Determine the noise in the difference image within the chosen region,  $\sigma_{\text{diff},d}$ , by using the IRAF routine `imstat`.
6. **For all pairs of images**, use the IRAF command `imstat` to extract the median signal,  $N_{e,d}$ , within the chosen regions for each pair of images. You can choose to do this for one of the images in each pair, or for both images and take the average of the two values.
7. Subtract the signal of one image from the other in each pair of images (Tip: use IRAF to create two lists of filenames, one for each image in a given pair. Then use the IRAF command `imarith` to subtract one from the other. Be careful to do the subtraction for images with the same exposure time.)

**For all pairs of images**, use the IRAF command `imstat` to extract the noise in the difference image within the chosen region,  $\sigma_{\text{diff},d}$ , by using the IRAF routine `imstat`.

#### 4.5.3 Tasks and discussion points for the protocol

- Find and discuss the photon noise, the read-out noise, and the PRNU noise for one flat image. Which noise dominates? Explain.
- Plot the variance of the signal versus the signal itself for all measurements with increasing exposure times in the I-filter and extract the electron sensitivity  $\kappa$  using eq. 23. Explain what this plot means.
- Calculate the electron sensitivity  $\kappa$  using eq. 19 and explain discrepancies with previous method. Do the calculation for just one image with average counts  $\sim 30\,000$  ADU.
- Discuss the quality of the analogue digital converter.

## 5 Color Magnitude Diagram

In this section you will use either your own KING data or archival images of the Hubble Space Telescope (HST) of the globular cluster BS90<sup>14</sup> to produce a color magnitude diagram that will allow you to estimate the distance, age, and metallicity of the cluster.

### Overview of the tasks

1. Determine the zero point for each image (see section 5.1)
2. Perform PSF fitting for each image (see section 5.2)
3. Cross-match the PSF fitting results (see section 5.3)
4. Plot the CMD and fit isochrones to it in order to estimate the distance, age, and metallicity of the globular cluster (see section 5.4)

### 5.1 Zeropoint calibration

As for all physical measurements, a careful calibration is essential for the detailed analysis of an astronomical observation. It is necessary to calibrate every measurement to a standard scale, since each observational facility and detector will have different characteristics. For astronomical observations this is the apparent magnitude scale. In order to get the zero-point magnitude we have to compare the counts of standard stars<sup>15</sup> in the Hubble images with reference values of the apparent magnitude from an astronomical data base called SIMBAD. For this purpose, open the V and I image of BS90 with ds9 and overplot one of the images with the catalog "Cool evolved stars in SAGE-SMC and SAGE-LMC (Boyer+, 2011)".

The catalogue can be loaded into ds9 as follows:

1. *Analysis* → *Catalogs* → *Search for Catalogs*
2. Set *Name or Designation* = J/AJ/142/103
3. Click *Retrieve*
4. One catalogue will show up in the list in the window. Select it and then click on *Catalog*
5. Now the objects will be overplotted on the image. On the pop-up window, you can sort the list after I-magnitudes, such that you can look at only those:  
*Sort* = *Imag*

---

<sup>14</sup>The images were taken with the HST filters F555W (V) and F814W (I).

<sup>15</sup>The reference stars we will use are not really standard stars, in the sense that they were calibrated themselves from true standard stars. This is due to our limited field of view, so the probability of a true standard star being located there is very low.

Now you have to select  $\sim 10$  stars for which you write down the V- and I- magnitudes and measure the counts in **both** Hubble images. To measure the counts you have to define a region around the reference star (with *Edit*  $\rightarrow$  *Region*; click into the image to create a region that can then be dragged to a different location). To get the right counts you have to make the region the right size, so that you get all the flux of the star without including any flux of another object nearby. If two stars are too close together choose another reference star instead. To get to the region statistics you have to double-click on the region and then go in the region menu to *Analysis*  $\rightarrow$  *Statistics*; *sum* gives you the counts and *error* the standard deviation. You can copy and paste the region to the other Hubble image and repeat the count measurement (you may have to slightly change the radius of the region).

After you have determined the counts and apparent magnitudes from the catalogue entry, you can compare your instrument magnitude with the CATALOG objects to calculate the individual zero points for all ten objects for both filters with the following equation:

$$\text{zeropoint} = m_{\text{CATALOG}} + 2.5 \log_{10} (\text{counts}) \quad (24)$$

Take the median to get your final zero point values for both filters and if necessary neglect extreme outliers.

## 5.2 PSF photometry with STARFINDER

In crowded regions for which the PSFs of different stars overlap aperture photometry does not work anymore. Therefore, we use STARFINDER, an IDL tool designed to perform PSF photometry that extracts a statistical PSF from the image and then tries to fit all stars in the image with that PSF.

To extract a PSF from the image STARFINDER needs the position of  $\sim 10 - 30$  isolated, unsaturated stars. On a bounding box around the stars, it subtracts an average background, normalizes the peak intensity, and averages the PSFs of all selected sources, thus creating an average PSF for the entire image.

Next, it tries to detect all sources above a certain threshold above the background level. The background is estimated by dividing the image to smaller chunks and fitting a slanted plane to each of those parts. For the source detection, the background is subtracted from the image and all pixel groups above the threshold are taken as potential stars.

In an iterative process, STARFINDER tries to fit all potential stars with the PSF and subtracts the results of this fitting from the science image. After all stars are analysed and subtracted, the background is recalculated and subtracted from the original science frame, after which the next iteration begins (i.e., another fitting of the PSF to all potential stars of the new background-corrected science image). That way we can disentangle and correctly account for the flux of overlapping sources.

However, this yields only the *instrumental magnitude* of these sources. To get the correct apparent magnitude, you have to use your calculated zero-point values from the previous section.

### 5.2.1 Using STARFINDER

STARFINDER is an interactive, widget-based IDL program. The following step-by-step tutorial will guide you through the photometry with STARFINDER.

#### Startup

1. start IDL from the console with `idl`
2. type `device, decomposed=0` to set IDL to the correct graphic mode
3. `xstarfinder` will start the graphical user interface (gui)
4. In STARFINDER, load a fits-file via `IMAGE ⇒ LOAD...`
5. You might want to change the (b/w) color scale to see the stars: `display ⇒ options`; also reverse the scale to be able to see the black cross-hair used for selecting stars

#### Determination of Noise

1. estimate the noise via `IMAGE → NOISE → compute`
2. within `NOISE`: you want STARFINDER to evaluate the noise from the data, taking the photon noise into account. Use the following settings:
  - `data=yes`: this computes a minimum noise threshold
  - `photon noise=yes`: this computes the noise for each pixel above the minimum noise threshold assuming Poissonian statistics
  - `Electrons/ADU = 2204 (V-Filter), 2316 (I-Filter)`
  - `Number of exposures=1`: Even though the Hubble images are composed of different exposures, this is already taken into account in the `Electrons/ADU` values
3. calculate the Gaussian noise with the standard parameters and plot the noise distribution in a histogram. You can also investigate the noise map with `ds9` after saving it.

The noise always has to be determined first since in the PSF fitting we will then use a threshold setting relative to that noise. So **if you have to restart starfinder for any reason you also have to repeat the noise determination!**

#### Determination of the PSF

1. in order to extract the PSF you need to know the size of the PSF; use logarithmic scaling in ds9 to find the radius that contains all the flux of a star
2. *PSF*  $\rightarrow$  *extract from image*
3. set the diameter of the output PSF<sup>16</sup>. The PSF size (in pixel) should neither be too small nor too big. Use ds9 to get a good estimate for the PSF size. You need not set the saturation limit as this has already been accounted for by the reduction of the Hubble images.
4. *Processing...* will let you select PSF stars; make sure to select isolated stars in order to reduce the contamination of your averaged PSF. Take a mix of medium bright stars (don't select the very brightest stars, be careful especially for the I-Filter)
5. STARFINDER will show you zooms of all selected PSF stars; only accept the best stars in order to obtain the best possible PSF. It is important that the brightest pixel is in the center. Discard all stars which are offset from the center or show complex substructure (double peaks, etc.).
6. After having checked all stars, repeat the procedure in this way: set the PSF size to approx. 50 pixels, then just click again *Processing*, and answer *yes* if asked if you want to use the same stars again. It then just re-computes the PSF for you, using the same stars as before.
7. You can look at the PSF with *Display PSF*. Adjust the display settings to see also the faint halo (e.g., `stretch=square root`, `colortable=Sternspecial`, `Min=0.0`)
8. exit the window used to obtain the PSF and save the list of stars used
9. save PSF (*PSF*  $\rightarrow$  *save*) and examine it in ds9; make sure the normalization did not fail, e.g., by checking the sum of pixel values in a rectangular region covering the whole PSF image
10. to improve and optimize the PSF, use *PSF*  $\rightarrow$  *Post processing*  $\rightarrow$  ...; *Halo smoothing* lets you do a radial smoothing of the PSF, *Support* lets you define a circular mask for the PSF. **Important: Normalize the PSF afterwards: *PSF*  $\Rightarrow$  *normalize***)

Sometimes the computed PSF shows artefacts in the upper right corner. If that happens re-do the selection of stars, but omit very faint ones. You might still see pixelation effects in the upper right corner, but these can be removed with the *Post processing* optimization tools. If the artefacts are too strong, just exit `starfinder` and restart the process (don't forget to recompute the noise first!)

### Determination of stellar flux by PSF fitting:

---

<sup>16</sup>The *Box size for background estimation* corresponds to the radius that contains all flux.



1. do iterative PSF fitting → *Astrometry and Photometry*
2. you can set a detection threshold, above which the routine will search for stars and fit the PSF to determine the counts. If you set the keyword "relative to noise", the routine will understand the detection threshold as multiples of the noise value at a certain pixel, which you have calculated in one of the previous steps. It is possible to do multiple iterations separated by a comma; use e.g. "3.,3."; this will re-determine the background after the first run of the search by subtracting all stars which have been found. It will then conduct a new search with the improved background model.
3. the correlation threshold lets the user reject stars for which the fitted PSF had an unsatisfactory correlation to the data; the standard of 0.7 is fine, but lower values (0.3 - 0.5) will give you many more stars (and thus also much fainter stars will be present in the resulting CMD).
4. take the noise into account
5. *Processing* will start the iterative PSF fitting

After the PSF fitting is done **make sure to save your output list before closing the window!** You can display all products of the analysis (the background model, a map of the detected stars, etc.) in the main window under *Display* → *Select data*.

### 5.3 Cross-match the PSF fitting results

For the CMD we plot the V vs. the V-I magnitudes, which means that only stars that were found in both images by STARFINDER can be used. To cross-match the two lists of the PSF fitting results you can use the Python script `matchstars.py`. Before running it you have to supply the relevant information to the configuration file `_config_matchstars.py`. The script automatically subtracts your determined zero points from the V and I magnitudes to produce the correctly calibrated apparent magnitudes in V and I.

### 5.4 Plotting the CMD

For plotting the CMD (V vs. V-I) and overplotting it with a set of theoretical isochrones you can use the Python script `cmdplot.py`. Before running it you have to supply the relevant information to the configuration file `_config_cmdplot.py`. Determine which isochrone fits the distribution of stars best by playing around with the age and metallicity values. You also have to determine the right shift in the V axis, which will then give you the distance to the cluster.

#### 5.4.1 Tasks and discussion points for the protocol

- Briefly discuss your settings and results for the zero point determination and the PSF fitting.

- Include a plot of your CMD with the best-fitting isochrone(s) and discuss the results of your distance and age determinations (e.g., comparison to literature values).

## 6 Scientific observations

In the steps described in the last section you have analysed the technical aspects of the detector and should have verified that the properties of the instrument are suitable for astronomical research, so that you can now proceed to take your own observations. However, due to the generally unfavourable weather conditions on the Königstuhl this may not be possible. If that should be the case, your supervisor will instead provide you with archival data to work with.<sup>17</sup>

### 6.1 Tasks

- Find a suitable globular cluster for the observations.
- Observe the globular cluster and relevant calibration data in two filters.

### 6.2 Execution of the observations

An astronomical observation has to be planned carefully in advance. To decide on which cluster to observe by you have to consider its position on the sky during the possible observation time. It is advisable to make a detailed plan of all the steps needed for the observation to allow a smooth work flow during the night and avoid wasting precious telescope time. You should think about the observing method to optimize the signal to noise and eliminate artefacts in the raw images.

Before the actual observations can be performed the telescope has to be focused. There are two buttons in the console for the telescope controls changing the position of the secondary mirror and thus the focus. Point the telescope to a clear part of the sky, make a test exposure, display the image on the computer and check whether you find an appropriate number of stars in the image. If that is the case set the focus to an arbitrary initial position and increase/decrease the focus for subsequent exposures. Write down the focus positions in your protocol. Take care to change the focus position only in one direction as the positioning mechanism exposes the behaviour of a hysteresis. With the IRAF task `starfocus` you can then analyze the images and determine the optimal position of the focus.

For the calibration of the magnitudes you also need observations of standard stars for all the filters with which you observed the globular cluster. Don't forget these as otherwise all your measurements are useless! Your supervisor will be able to help you find a suitable field for standard stars.

### 6.3 Analysis

#### 6.3.1 Introduction

The majority of the visible stars are in the hydrogen burning phase and thus populate the main sequence in the Hertzsprung-Russell-Diagram (HRD). In a stellar

---

<sup>17</sup>It is very common in astronomy to use archival data and many new discoveries have been made from the re-analysis of “old” data.

population with a defined age, like a globular cluster (GC), it is possible to deduce its evolution history, its age and its distance from the form of its HRD. Producing an HRD in practice is rather difficult since both absolute brightness and spectral type of a star are often not exactly known. In observational astronomy it is therefore common to use a color-magnitude-Diagram (CMD) in which the apparent magnitude, e.g.  $V$ , is plotted against the color, e.g.  $B-V$ . These values are possible to determine directly from observations. This is the goal of this experiment. According to the time of year, ergo, the visibility on the sky and some properties (size, magnitude) one GC is chosen by the assistant. Its images are then taken with the 70cm KING telescope in two wavelength ranges,  $B$  and  $V$  (corresponding to the Johnson-System). After “reducing” the images to their scientific content and their evaluation, the measured instrumental magnitudes of the stars in the GC can be translated to the standard apparent magnitudes which produce its CMD. By fitting the theoretical model-isochrones (“lines of equal age”) to the plotted CMD, the age and the distance of the GC can be determined.

### 6.3.2 Data acquisition

Before taking images of the GC some preparatory work is necessary. In general, “raw” images coming from the telescope have instrumental defects which we have to correct. They are removed later from the images, enabling an exact calibration of the photon fluxes across the array. For that, images of two kinds have to be acquired - “Bias” and “flat-field”. In the following it is described how to do that.

### 6.3.3 Bias

To measure the bias perform 5 integrations of 5 seconds each with the shutter closed. Pay attention to the position of the shutter during the integration. Is it necessary to measure the bias with each filter?

### 6.3.4 Flatfield

For the sake of redundancy and in order to remove single pixels saturated by cosmic rays, take at least 5 dome-flat exposures with each filter (see section 4.3). A “master flat-field” can then be constructed by combining these single flat-fields and calculating the median for each pixel. Each scientific exposure has to be divided by the normalized master-flat to correct for its small- and large-scale pixel-to-pixel variations.

If the weather and time should allow it, another method to perform flatfield calibration is to make images of the twilight sky when the Sun is already below the horizon but the sky is still not completely dark. The available period for doing this is relatively short - if it is still too bright the CCD saturates immediately; if it is already too dark, the low brightness of the sky will necessitate longer integration times, causing stars to appear on our flatfield image. Nonetheless, the sky-flatfield is preferable to the dome-flatfield since the CCD is illuminated in the same way as in the scientific exposures. It also avoids possible effects introduced by the

artificial dome lights, such as weak patterns of scattered light and non-uniform illumination.

Sky-flatfields are performed analogous to dome-flatfields. Even though the twilight sky may seem homogeneous to our eyes, it is probable that the CCD will detect some bright stars. To avoid detecting them always with the same pixels, move the telescope after each exposure approx. 10 arcsec in the same direction along one coordinate. When deciding with which filter to start (considering the limited time), take into account that the colour of the sky is blue.

### 6.3.5 Finding the focus

After we have taken the necessary calibration data, we have to set the focus, i.e., align the position of the focal plane of the telescope with the plane of the CCD-Chip. For that we slide the secondary mirror along the optical axis by pressing the + or - "focus" button on the control console. But first, we should make a short "acquisition image" of the night to make sure that a couple of sufficiently bright stars are visible within the field of view. If that is the case, we can perform a series of 7 measurements, starting with one position of the secondary mirror and scanning a value range of approx. 20 (as displayed on the control console). Write down which value displayed on the control console corresponds to which image name. That is necessary to find out which position of the secondary mirror corresponds to the best image. The optimal focus position can be calculated with the IRAF task "starfocus" which takes the images and measures the point-spread function (PSF) width of stars (selected interactively) in each image and makes a parabolical fit to the values. This has to be done for all filters that will be used in the measurements.

After the focus is set, the actual imaging of the GC can be performed. For that, point the telescope to the sky coordinates of the GC. Because the pointing accuracy of the KING telescope is not perfectly calibrated there is a small offset between the coordinates displayed on the control console to the real sky coordinates. Therefore, we first have to make a test image to find the necessary shift we have to apply to the coordinates so that our object will be centered in the image. This test image is also useful for deriving the integration time for a single exposure with the given filter. Given the linearity of the CCD, an integration time should be chosen at which the central (= brightest) region of the GC will be at the upper end of the linear range of the detector. This will optimise the efficiency of the observations since the time needed to read out the CCD is relatively long (approx. 1 min for resolution 2048x2048) and independent of the exposure time.

Finally, we can start to image the GC. In order to avoid the negative effects of observing the same sky area with the same pixels (possibly "bad pixels" or pixels locally saturated by cosmic rays), we use an observing method in which the object is moved ("dithered") across the array by a few arcseconds after each exposure, so that in each image the pixels observe a different part of the sky or object. Hence, for every new exposure, the telescope has to be repositioned by approx. 10 arcsec according to the chosen observing pattern. This pattern can be a triangle,

a rectangular, a spiral, a cross, etc.

The derived apparent magnitudes can now be plotted in a colour-magnitude diagram (e.g.,  $V$  vs.  $V-R$ ) and evaluated with the help of model isochrones. Shifting the isochrones along the  $V$ -axis allows to choose the one that fits the CMD best, which gives the estimated age of the GC. Since the isochrone units are absolute magnitudes, the comparison of the positions of the fitted isochrone on the vertical axis allows to calculate the distance modulus  $m-M$ . Given the weather conditions on Koenigstuhl, usually the quality of the resulting CMD is not perfect. To achieve better fitting constraints, it is recommended to make separate histograms of  $V-R$  for a certain slice in  $V$  to identify the average value of  $V-R$  and its dispersion.

## 7 Data Analysis

### 7.1 Raw data reduction

Before doing photometry, we have to reduce the raw data of our observations. For this purpose, calibration exposures should have been taken at the day of the observation. As the behaviour of the detector may vary with physical conditions (e.g. temperature, filter, pointing, etc.), it is important to take individual calibration exposures for every scientific observation. There are two types of calibration images relevant for this experiment: bias and flat field.

If the observations have been taken in dithering mode the bias-subtracted and flat-field-divided images have to be matched. This is done similarly to the method used for obtaining the master flat field, with the difference that the images have to be aligned first.

After these principal reduction steps have been performed, any well-defined detector background should have been removed and one can start to think about the scientific analysis - which, in our case, is performing photometry on the astronomical objects in our image.

#### 7.1.1 Execution

The bias subtraction and the flat field division can be performed by using the `imarith` task in IRAF:

```
vocl> imarith science_V_0000.fits - bias science_V_0000_b.fits
vocl> imarith science_V_0000_b.fits / flat_V science_V_0000_bf.fits
```

If several exposures were performed in one filter the images have to be shifted and aligned before they are combined. This can be done with the task `imalign`:

```
vocl> imalign @science_V_bf_list.txt science_V_0000_bf.fits
          coordinate_list.txt @science_V_bfa shifts=offset_list.txt
vocl> imcombine @science_V_bfa science_V combine=median
```

Here, the parameters after the main command define the list of input images, a reference image to which the input images are aligned, a text file containing a list of coordinates of objects in the reference image used for the alignment process, the name of the output files, and a first estimate of the offsets, where `offset_list.txt` is a file containing the offset of the files listed in the input list. The last option is sensible if the offset between the frames is more than a few pixels. The list of objects can be compiled selecting objects with `imexam` and the offset file can be calculated from the coordinate differences of a star in every frame.

You should now have two images of the star cluster and two images containing the standard stars (if they are not already contained in the same frame as the star cluster) in the two different bands for the further data analysis.

## 8 Command line commands for reading out the CCD

The CCD can be controlled from the command line prompt on the *clearsky* computer. The main command is `ccdread` followed by certain parameters.

### 8.1 Resetting the electronics

```
> ccdread -R -I -C 1
```

**-R** reset the electronics

**-I** initialize the electronics

**-C 1** short circuit the pixels

### 8.2 Taking a dark exposure

```
> ccdread -C 0 -b 2 -g 5 -T -f dark.fits -E 60  
          -o "dark_current" -u "name1 name2" -O -C 1
```

**-C 0** ...

**-b 2** set the binning factor to 2, i.e. 2 pixel in x-direction and 2 pixel in y-direction will be binned into one single pixel.

**-g 5** set the detector's gain factor to 5

**-T** write the temperature into the header of the .fits image file

**-f** specify the full file name hereafter

**-E** specify the integration/exposure time in seconds hereafter (shutter will remain closed!)

**-o** specify the object's name hereafter

**-u** specify the observer's name hereafter

**-O** read out the CCD

**-C 1** short circuit all pixels



### 8.3 Taking a flatfield or science exposure

```
> ccdread -C 0 -b 2 -g 5 -T -F filename -e 60  
          -o "flatfield" -u "name1 name2" -O -C 1
```

**-C 0** ...

**-b 2** set the binning factor to 2, i.e. two pixels in x-direction and two pixels in y-direction will be binned into one single pixel.

**-g 5** set the detector's gain factor to 5

**-T** write the temperature into the header of the .fits image file

**-F** specify the basis of the file name; a running number will be attached automatically, e.g., filename0001.fits

**-e** specify the integration/exposure time in seconds hereafter (shutter will be opened!)

**-o** specify the object's name hereafter

**-u** specify the observer's name hereafter

**-O** read out the CCD

**-C 1** short circuit all pixels

## References

- Boyle, W. S., & Smith, G. E. 1970, Charge Coupled Semiconductor Devices, Bell Sys. Tech. J., 49, 587
- Léna, P., Lebrun, F., & Mignard, F. 1998, Observational astrophysics.
- Milone, A. P., Bedin, L. R., Piotto, G., et al. 2008, The ACS Survey of Galactic Globular Clusters. III. The Double Subgiant Branch of NGC 1851, ApJ, 673, 241
- Stetson, P. B., & Harris, W. E. 1988, CCD photometry of the globular cluster M92, AJ, 96, 909
- Unsöld, A., & Baschek, B. 2002, Der neue Kosmos. Einführung in die Astronomie und Astrophysik
- Yi, S. K., Kim, Y.-C., & Demarque, P. 2003, The  $Y^2$  Stellar Evolutionary Tracks, ApJS, 144, 259